A&A manuscript no.
(will be inserted by hand later)

Your thesaurus codes are:
03 (11.03.4 Cl 1613+3104; 11.03.4 Cl 1600+4109; 11.16.1; 11.19.5)

ASTRONOMY
AND
ASTROPHYSICS
16.1.2018

The population of galaxies in the distant clusters Cl 1613+3104 and Cl 1600+4109⋆

R. Vílchez–Gómez[1], **R. Pelló**[2], **and B. Sanahuja**[1]

[1] Departament d'Astronomia i Meteorologia, Universitat de Barcelona, Av. Diagonal 647, E–08028 Barcelona, Spain
[2] Laboratoire d'Astrophysique de Toulouse, URA 285, Observatoire Midi–Pyrénées, 14 av. Édouard Belin, F–31400 Toulouse, France

Received 1995; accepted 1996

Abstract. We study the photometric properties and content of the distant clusters of galaxies Cl 1613+3104 ($z = 0.415$) and Cl 1600+4109 ($z = 0.540$). The former is a rich, concentrated cluster which shows a strong evidence for segregation in luminosity and color. Its population of galaxies separates into two different kinds of objects: a red population compatible with the colors expected for E/S0 galaxies located preferentially in the central part of the cluster, and a sparse blue population explained in part by the presence of normal S/Im galaxies, which is much less concentrated. In the case of Cl 1600+4109, there is a lack of E/S0 galaxies and the population is mainly made up of S/Im galaxies, without any evidence of segregation in magnitude or in color. Both clusters exhibit an important fraction of blue objects, increasing with magnitude. This result is due in part to the presence of normal S/Im galaxies, and also to extremely blue objects probably undergoing an episode of intense star-formation.

Key words: Galaxies: clusters: individual: Cl 1613+3104 and Cl 1600+4109 – Galaxies: photometry

1. Introduction

Photometry of rich clusters of galaxies at high redshift remains one of the most important tools to understand the evolution of galaxy populations in dense environments. The discovery of a large fraction of blue galaxies in rich clusters has been understood as evidence for a strong, recent evolution of galaxies in clusters (Butcher & Oemler 1984, hereafter BO; Sharples et al. 1985). The interpretation of this blue excess is a difficult challenge because the galaxy content varies from cluster to cluster. Dressler et al. (1985) suggested that it can arise from several reasons: different initial conditions, a difference in the time scales for cluster formation and/or environmental influences. The presence of luminosity and color segregation in nearby clusters (Capelato et al. 1980) as well as in high redshift clusters (Mellier et al. 1988) is often interpreted in terms of dynamic friction and environmental influence (galaxy-galaxy and galaxy-ICM interactions). Nevertheless, it is not still clear to what extent these properties are innate or the result of later evolutionary processes. Dressler & Gunn (1992) published a paper on the photometry and spectroscopy of seven clusters in the redshift range $0.35 \leq z \leq 0.55$, including a thorough discussion on the statistical properties of the sample. Such studies are crucial to an understanding of the evolutionary processes that take place in clusters. Recently, Dressler et al. (1994a,b) and Coutch et al. (1994) studied the morphology of the blue galaxies in clusters at $0.3 \lesssim z \lesssim 0.4$, using HST images. They found that the blue objects are predominantly disk-dominated or irregular galaxies, involved in merger or interaction processes. Thus, it is important to enlarge the sample of well known high and medium redshift clusters, and photometry allows to study a larger sample of galaxies than spectroscopy.

Cl 1613+3104 ($\alpha_{1950} = 16^{\rm h}13^{\rm m}49\overset{\rm s}{.}2$, $\delta_{1950} = 31°4'57\overset{''}{.}0$; $l = 50\overset{\circ}{.}58$, $b = +45\overset{\circ}{.}56$) is a mid-redshift rich cluster, which exhibits X-ray (Henry et al. 1982) and radio emission (Jaffe 1982). Its redshift ($z = 0.415$) was obtained by Sandage et al. (1976) from the spectrum of the first-ranked galaxy. Vílchez–Gómez et al. (1994) reported the existence of a diffuse light extending up to 265 $\rm h^{-1}$ kpc from its center, associated with a stellar component immersed in the gravitational potential of the cluster. Cl 1600+4109 ($\alpha_{1950} = 16^{\rm h}\ 0^{\rm m}\ 23\overset{\rm s}{.}0$, $\delta_{1950} = 41°\ 9'\ 39\overset{''}{.}0$; $l = 65\overset{\circ}{.}21$, $b = +48\overset{\circ}{.}72$) is another mid-redshift cluster ($z = 0.540$;

Send offprint requests to: R. Vílchez–Gómez

⋆ Based on observations made with the 3.5 m telescope of the Centro Astronómico Hispano–Alemán de Calar Alto in Almería (Spain), operated by the Max-Planck-Institut für Astronomie, Heidelberg (Germany), jointly with the Spanish Comisión Nacional de Astronomía

Henry et al. 1982) included in the sample of Gunn et al. (1986), whose population of galaxies has not been studied to date. It is not a strong X-ray emitter: its upper limit for the X-ray emission is 1.6×10^{44} erg s^{-1} in the 0.5–4.5 keV range (Henry et al. 1982). The database used here comes from the photometric survey by Pelló & Vílchez–Gómez (1996), hereafter referred as Paper I.

The layout of this paper is the following. A summary of the observational procedure is presented in Sect. 2. Section 3 reviews the methods used in the analysis of the photometric catalogs and the results obtained are given in Sects. 4 and 5. In Sect. 6 we discuss these results and we present the conclusions of this work. We assume $H_0 = 50$ km s^{-1} Mpc^{-1} and $q_0 = 0.1$ in a standard Friedmann cosmology.

2. Summary of the photometric observations

The observations reported here were carried out in two different runs (in May 1987 and July 1988) at the F/3.4 prime focus of the 3.5 m telescope of the *C.A.H.A* (Calar Alto, Almería, Spain). All the details can be found in Paper I. The detector used was an RCA CCD, with an equivalent field of $4\farcm4 \times 2\farcm8$ and a pixel size of $0\farcs506$. The filters used were Johnson B and Thuan–Gunn g and r (Thuan & Gunn 1976), with effective wavelengths of 4416, 4892 and 6681 Å, respectively. These filters avoid the most important emission lines from the sky, which produce a strong fringing in RCA CCDs. As a consequence, the S/N of the images is improved and the detection level is much better. A more important reason to select these filters refers to the redshifts of both clusters and the predictions obtained by the synthetic models of spectro-photometric evolution (Bruzual & Charlot 1993; Rocca–Volmerange & Guiderdoni 1988). The magnitudes derived from these filters refer to fluxes emitted at 3120, 3457 and 4721 Å in the rest frame of Cl 1613+3104, and at 2867, 3177 and 4338 Å in the rest frame of Cl 1600+4109. The main feature in the spectrum of galaxies in the optical range is the discontinuity at 4000 Å, which is located between filters g and r for galaxies at these redshifts ($z \sim 0.4$–0.5). Thus, the g − r color gives a good measure of the relative spectral flux before and after the discontinuity, and it is a useful tool to discriminate between cluster and field galaxies. Furthermore, for the same redshift range, the B filter samples a region of the spectrum very sensitive to star formation activity. These filters allow to obtain some reliable information about the population of galaxies and the star formation history in these clusters.

For each filter and cluster, we took equivalent exposures on an empty field near the cluster ($10'$ southward from the center of Cl 1613+3104, and $7'$ southward and $7'$ westward from the center of Cl 1600+4109). These images were reduced in the same way as the cluster ones. The comparison field allowed the statistical correction of the cluster content for the contamination due to foreground and background objects within the same line-of-sight. Table 1 of Paper I gives the main characteristics of the photometric CCD images of the clusters and the respective comparison fields used here. To be sure that the comparison fields are not contaminated by the presence of other clusters of galaxies, we used Zwicky et al.'s catalog (1961–1968) to determine the position of the comparison field with respect to the cluster. An estimate of the foreground reddening was obtained using the maps of Burstein & Heiles (1982) and the Galactic extinction law (Cardelli et al. 1989). The reddening correction to each color is less than 0.01 mag in all the cases, which is consistent with the colors obtained for objects identified as stars (Paper I). Thus, we did not introduce the reddening correction in our analysis because it is much lower than the absolute photometric accuracy for the brightest objects in the field.

3. Data analysis

The first goal is to estimate the distribution of galaxies in spectro-morphological types through the observed distribution in colors. We used Bruzual's code (Bruzual & Charlot 1993) for the spectro-photometric evolution of galaxies, in order to obtain the SEDs corresponding to 6 spectro-morphological types: E/S0, Sa, Sbc, Scd, Im and a single starburst. The IMF was taken from Miller & Scalo (1979), with a lower and upper cutoff masses of 0.1 and 125.0 $M_\odot$ respectively. For each morphological type, we calculate the evolution of colors as a function of the redshift. The present age of galaxies is assumed to be 15 Gyr, which corresponds in this cosmological model to a galaxy formation redshift of 5.3. The real transmission functions of the photometric system constituted by the filters plus the CCD response are taken into account to derive the k and e corrections to magnitudes and the synthetic colors. In this way, observations can be easily compared to color predictions and undesirable color effects are avoided. The fraction of blue objects, with a definition which is similar to that given by BO, is also determined.

The contamination due to fore and background galaxies has been evaluated as a function of the different magnitudes and colors by means of the comparison field. This is a key point because the population of cluster galaxies appears as an excess with respect to the field population. In particular, the Schechter luminosity function (Schechter 1976) is used to fit the distribution of galaxies in B,

$$\mathrm{n}(L)\mathrm{d}L = \mathrm{n}^* \left(\frac{L}{L^*}\right)^{\alpha} \mathrm{e}^{-L/L^*} \mathrm{d}\left(\frac{L}{L^*}\right), \qquad (1)$$

through a Gauss–Newton χ^2 minimization algorithm.

The 2D distribution of galaxies has also been studied. To evaluate the degree of central concentration of the clusters, we computed the concentration index (C), R_{30} and N_{30}, as defined by Butcher & Oemler (1978). Nevertheless, these parameters need an accurate determination of

Fig. 1. Distribution in absolute B magnitude and colors of objects in the field of Cl 1613+3104, before (white histograms) and after (black) correction for contamination using the comparison field: **a** Isophotal B magnitude, **b** B − r, **c** g − r. In b and c, only objects brighter than the completeness magnitude in g have been considered. $\pm 1\sigma$ error bars at the bottom of the histograms correspond to the net corrected population

the extent of the cluster and a good correction of the fore and background contamination. Therefore, we also used the average central density, $N_{0.5}$ (Bahcall 1981), which is very easily determined and almost insensitive to these errors.

The projected densities of these clusters (number of galaxies per surface unit or surface brightness) were fitted using a Gauss–Newton χ^2 minimization algorithm to the analytic profile given by:

$$\sigma(r) = \sigma_0 \left(1 + \left(\frac{r}{R_c}\right)^2\right)^{-\alpha}. \quad (2)$$

This law corresponds to the Hubble profile when $\alpha = 1$. Unless otherwise indicated, the sample used is defined within the completeness limit in magnitude. The center of the cluster is defined as the optical barycenter of the central brightest galaxy, when there is only one (Cl 1600+4109), or as the optical barycenter of the whole central group of galaxies (Cl 1613+3104).

The existence of subclustering and the presence of segregation in luminosity and color can be detected performing the angular-separation test (λ_n-method) proposed by Hickson (1977), as developed by Capelato et al. (1980). This method introduces a set of length scales defined by:

$$\lambda_n = \left(\frac{1}{N_p} \sum_{i>j} r_{ij}^n\right)^{1/n}, \quad (3)$$

where N_p is the number of pairs of galaxies and r_{ij}, the angular separation between galaxies i and j. The λ_n values are calculated over successive magnitude or color intervals, to check for the existence of segregations in luminosity and color. This test has the advantage of being independent of the position of the center and the shape of the cluster. We adopted the definition of *segregation* given by Capelato et al. (1980). We used λ_1 and λ_{-1} and the field has been limited within a circle smaller than the image size to avoid the edge effects. The size of the different magnitude or color intervals were imposed in such a way that each one contains approximately the same number of galaxies.

4. Cl 1613+3104

4.1. The population of galaxies

Figure 1 shows the histograms in absolute magnitude for the B filter as well as the distribution in colors, before and after correction for contamination using the comparison field. Only objects unambiguously identified as stars have been excluded from the sample (following the method explained in Paper I). The luminosity function in B has been derived according to Eq. (1), using the same k correction for all the objects (assuming that they are all E/S0 galaxies). The fit gives: $n^* = 40 \pm 20$, $\alpha = -0.8 \pm 0.6$ and $M_B^* = -20.8 \pm 0.8$ (reduced χ^2 is 3.75, with 3 degrees of freedom). These values are compatible with those derived by Colles (1989) for a sample of 14 rich and nearest ($z < 0.15$) clusters, also using a χ^2 minimizing method. If we assume $\alpha \equiv -1.25$, then, $n^* = 19 \pm 6$ and $M_B^* = -21.4 \pm 0.5$ (the reduced χ^2 is 1.78 with 4 degrees of freedom), which are very close to the values obtained by Colles, fixing also α. The distribution of galaxies in colors clearly shows a double peak in g − r. This configuration divides the sample of galaxies into blue ($0.0 \lesssim g-r \lesssim 0.7$) and red ($1.0 \lesssim g-r \lesssim 1.5$) populations. The separation into populations is less evident in B − g, which shows only one broad peak centered around 0.4. In B − r, the sample of galaxies shows an important fraction of blue galaxies ($B-r \lesssim 1.8$) and the presence of a red population ($B-r \gtrsim 2.0$).

Figure 2 shows the color–magnitude diagrams for the cluster, where the separation between stars, galaxies and unidentified objects has been introduced according to Table 2 in Paper I. The red sequence for the distribution of E/S0 galaxies is less relevant than in other clusters (for example, compared with BO or Dressler & Gunn (1992), for the same type of clusters). An important blue population appears in these diagrams, as preliminary evidence in favor of an important fraction of star–forming galaxies. This population is examined below.

Fig. 2. Color–r magnitude diagrams in the field of Cl 1613 +3104: **a** (B − r), **b** (g − r). The (B − r)(r) locus of B_{com} and the (g − r)(r) locus of g_{com} are given by solid lines, whereas r_{com} is shown by a dashed line. Galaxies are plotted as black dots, whereas stars and unidentified objects appear as stars and plus signs, respectively

Table 1 gives the distribution in spectro-photometric types of objects in excess in the cluster field with respect to the comparison field. Spectrophotometric types are determined as boxes on the color-color plane. Extremely blue objets (EB) are objects bluer than the values predicted for an Im type at the cluster redshift. Again, only objects identified unambiguously as stars have been excluded from the sample. Figure 3 shows the color-color distribution of objects for three intervals in r magnitude, where we superimposed the synthetic sequence of morphological types derived using Bruzual's code. The population of blue galaxies in the color–color diagram increases with the magnitude, as shown in Table 1. Nevertheless, to obtain the absolute distribution in spectro-morphological types from these values, the sample must be limited within the magnitude of completeness for *all* the filters (see discussion in Sect. 6).

Table 1. Distribution of the excess of galaxies in the field of Cl 1613+3104 with respect to the comparison field.

	E/S0	S/Im	EB
(B − r)	[1.8, 2.9]	[0.6, 1.8]	< 0.6
(g − r)	[1.2, 2.0]	[0.4, 1.2]	< 0.4
All	27%	28%	45%
$r \leq r_{com}$	44%	33%	23%
r ≤ 22	75%	22%	3%

All these data suggest the following question: How do classify BO "blue" objects identified in this field according to this scenario? Following BO, a galaxy is "blue" when the B − V color in its rest frame is at least 0.2 mag bluer than the center of the E/S0 peak, and the fraction of blue galaxies, f_B, is obtained as the fraction of such galaxies with respect to the total corrected population of galaxies, with $M_V < -20$ within R_{30}. Then, the total number of objects with $M_V < -20$ (equivalent to r < 21.8 for elliptical galaxies at $z = 0.415$) is only 60 within the cutoff radius of the cluster (see Sect. 4.2), and 21 within R_{30} (= 42″, Sect. 4.2). Eight of them have B − g colors 0.2 mag bluer than a typical E galaxy. The equivalent values in the comparison field within R_{30} are 8 and 3, respectively, so the contamination level is about 40–50%. The fraction of blue objects inferred in this way is $f_B = 0.4 \pm 0.2$, which is higher than the typical value and only marginally compatible with the z–f_B relation obtained by BO for a rich cluster at $z = 0.415$ ($f_B \sim 0.2$). This fraction increases if we redefine the fraction of blue objects by considering the sample within the completeness limit in g ($g_{com} = 24.25$) and within R_{30}. The total number of objects is 41, with a contamination level of about 40 to 50%. Among them, 22 are "blue" objects and the contamination level for this sample is also about 50%, so $f_B = 0.47 \pm 0.19$. 14 of these objects are compatible with stars according to their colors. The remaining objects are classified as follows, assuming that they are cluster members: 4 as S galaxies, 3 as Im galaxies and 1 as an extremely blue object.

Fig. 3. Color–color diagrams in the field of Cl 1613+3104 and in its comparison field. Three magnitude intervals have been considered: **a and b** r ≤ 22, **c and d** 22 < r < 24, **e and f** r ≥ 24. Objects are identified as in Fig. 2. The colors predicted for the different types of galaxies at $z = 0.415$, from E to Im, and the typical error boxes in each magnitude bin are also shown

4.2. The 2D distribution of galaxies

The shape of Cl 1613+3104 is basically circular with an ellipticity $\epsilon \simeq 0.15$ (defined as $\epsilon = 1 - b/a$, where a and b are, respectively, the major and the minor axes of the ellipse) and a position angle $\theta \simeq 100°$ with respect to the N–S direction (Vílchez–Gómez et al. 1994). This ellipticity is small enough to assume radial symmetry. The cluster core presents a compact group of 6 luminous galaxies (Fig. 1 in Paper I) within a radius of about 17″ (121 h^{-1} kpc) around the center, with magnitudes between r = 19.13 and r = 20.33.

Fig. 4. **a** λ versus r magnitude diagram in the field of Cl 1613+3104. **b** λ versus (g − r) diagram. **c** Magnitude segregation in two different color samples. **d** Color segregation in three different magnitude samples. All the bins contain, approximately, the same number of objects

Two partially overlapping images are available in r, one of them shifted 71″ with respect to the other. Therefore, as the spatial coverage is larger in r, we have used these images to estimate the concentration of the cluster. The equivalent image on the comparison field gives the zero point for the projected density of galaxies. We have calculated the cluster profile and we have defined the cutoff radius as the distance at which the projected density coincides with the density in the comparison field. The cutoff radius obtained is 101″ (718 h^{-1} kpc). The total number of objects inside this radius is 456, and 207 of which have a magnitude lower than the completeness limit in r (r_{com}).

The number of objects found for the comparison field, under the same conditions, is 264 and 90, respectively. Assuming that all galaxies are elliptical, the magnitude r_{com}= 24.0 is equivalent to $M_V = -17.8$, taking into account the distance modulus and the k+e correction. With this limit of magnitude, the concentration parameter derived is C = 0.36, with $R_{30} = 41''$ (292 h^{-1} kpc) and $N_{30} = 35$, indicating a highly concentrated cluster. If we take the limit in magnitude used by BO ($M_V = -20.0$, r = 21.8), we obtain a concentration parameter C = 0.52, with $R_{30} = 42''$ (298 h^{-1} kpc) and $N_{30} = 13$. In this case, the total number of objects in the cluster field is much lower: 60 compared to 16 in the comparison field. The central galaxy density, $N_{0.5}$, is 24 and the velocity dispersion, estimated from the empirical relation found by Bahcall (1981), is 1000–1200 km s^{-1}. All these results confirm that we are dealing with a rich, compact cluster.

The projected galaxy density profile can be derived by fitting the cluster profile according to Eq. (2): $\sigma_0 = 0.015 \pm 0.004$ gal arcsec^{-2}, $\alpha = 0.8 \pm 0.2$ and the core radius is $R_c = 21'' \pm 8''$ (150 ± 60 h^{-1} kpc). The radius at which the projected density reduces to $\sigma_0/2$ is $R_h = 25'' \pm 10''$ (180 ± 70 h^{-1} kpc). These radii are similar to the typical radii found for other rich clusters with similar redshifts, such as A 370 (Mellier et al. 1988).

The luminosity and color segregations are important in Cl 1613+3104. Figure 4 displays the values of the characteristic lengths for different magnitude and color bins. There is a segregation in luminosity (manifest for λ_{-1} in Fig. 4a) as well as a clear segregation in color (Fig. 4b). To check on the independence of these segregation effects, we have applied this method to different color and magnitude samples within the completeness limits in magnitude (Figs. 4c and 4d). The brightest and reddest objects are more concentrated because their characteristic lengths are systematically shorter than those for the faint, blue objects. In contrast, bright *and* blue objects appear anti-segregated, as expect for stars and foreground galaxies in this small field. If we select a sample of objects with the same λ, in the color range $0.75 \geq g - r \geq 1.8$, the luminosity segregation becomes evident (Fig. 4c). Conversely, a sample of magnitude-selected objects with the same λ, shows clearly a color segregation (Fig. 4d). So, these segregation effects are independent, at least up to $r \simeq 23$. Objects fainter than $r \simeq 23$ are quite uniformly distributed. Moreover, the red, luminous galaxies preferentially appear in the central part of the cluster. If we consider the magnitude and color distribution of objects brighter than r_{com} as a function of their radial distance to the central galaxy, galaxies lying within a radius of 15″ (107 h^{-1} kpc) from the center are redder and brighter than the outside population (the contamination expected in this region is lower than 20%). Figure 5 shows the contour plots of the projected number density of galaxies, for a red sample ($1.0 \lesssim g - r \lesssim 2.0$) and a blue sample ($0.0 \lesssim g - r \lesssim 1.0$), according to the distribution of galaxies in g − r (Sect. 4.1). The mean projected densities obtained over the cluster field for these two samples are 1.8×10^{-3} and 5.0×10^{-3} objects arcsec^{-2} respectively. These values can be compared to the equivalent ones in the comparison field: 0.6×10^{-3} and 3.4×10^{-3} objects arcsec^{-2} respectively. In conclusion, the red population is strongly concentrated around the center of the cluster (Fig. 5a) whereas the blue is uniformly distributed (Fig. 5b). Very similar 2D distributions are obtained by dividing the sample into bright ($r \leq 23$) and faint ($r \geq 23$) objects, which are fully compatible with the results shown in Figs. 5a and 5b for the red and the blue populations, respectively.

5. Cl 1600+4109

5.1. The population of galaxies

The number of objects detected in this field is lower than in Cl 1613+3104. 334 objects were found in the cluster field compared to 192 objects in the comparison field, so the excess of objects potentially belonging to the cluster is 142. For this reason, the analysis of the population of galaxies in this case is more difficult than in Cl 1613+3104. The distribution of these objects in absolute magnitude in B (a k correction for E/S0 galaxies was assumed) and colors B − r and g − r, before and after correction for contamination, is shown in Fig. 6. Most of the objects belonging to the cluster are beyond the completeness limits in magnitude: $24 \lesssim B \lesssim 27$, $24 \lesssim g \lesssim 27$ and $23 \lesssim r \lesssim 27$. A tentative fit of the luminosity function in B, according to Eq. (1), gives $n^* = 12 \pm 2$ and $M_B^* = -22 \pm 4$, with $\alpha \equiv -1.25$ (the reduced χ^2 is 4.3, with 1 degree of freedom).

The distribution of galaxies in colors takes into account all the objects detected, without introducing any selection in magnitude. These distributions, after correction using the comparison field, are rather irregular. Both the B − r and the g − r histograms show a broad distribution of blue objects ($1.0 \lesssim B - r \lesssim 2.5$ and $0.2 \lesssim g - r \lesssim 1.6$), with very few red objects ($B - r \gtrsim 2.5$ and $g - r \gtrsim 1.6$). Figure 7 shows the color–magnitude diagrams for this cluster. The morphological separation between stars and galaxies in this case is more difficult than in Cl 1613+3104 because the seeing and the linear sampling are poorer (Paper I). For this reason, we do not introduce a discrimination *a priori* between stars, galaxies and unidentified objects, neither in the cluster field nor in the comparison field. The E/S0 color–magnitude sequence is barely visible in this cluster.

Table 2 shows for different samples the excess of objects in the cluster field with respect to an empty field. Figure 8 shows the color–color diagrams of the cluster and comparison fields per bin in r magnitude. The importance of the blue population of galaxies in the color-color diagrams increases with magnitude (as for Cl 1613+3104).

Fig. 5. Isocontour maps of projected number density of galaxies: **a** red galaxies ($1.0 \lesssim g - r \lesssim 2.0$); 12 contours levels are shown for 1 to 13 times the mean projected density over the cluster field, starting at 1. **b** blue galaxies ($0.0 \lesssim g - r \lesssim 1.0$); the difference between two successive contour levels is 0.5 times the mean projected density over the cluster field, starting at 1. X and Y coordinates are in arcsecs with the cluster center at (80″, 130″). See comments in Sect. 4.2

Fig. 6. Distribution in absolute B magnitude and colors of objects in the field of Cl 1600+4109, before (white histograms) and after (black) correction for contamination: **a** Isophotal B magnitude, **b** B − r, **c** g − r. $\pm 1\sigma$ error bars at the bottom of the histograms correspond to the net corrected population

Fig. 7. Color–r magnitude diagrams in the field of Cl 1600 +4109 : **a** (B − r), **b** (g − r). The (B − r)(r) locus of B_{com} and the (g − r)(r) locus of g_{com} are given by solid lines, whereas r_{com} is shown by a dashed line. Galaxies are plotted as black dots, whereas stars and unidentified objects appear as stars and plus signs, respectively

Note that in this case the same warning comment as in Cl 1613+3104 is applicable concerning the absolute distribution in morphological types.

Table 2. Distribution of the excess of galaxies in the field of Cl 1600+4109 with respect to the comparison field.

	E/S0	S/Im	EB
(B − r)	[2.2, 3.3]	[0.6, 2.2]	< 0.6
(g − r)	[1.1, 2.3]	[0.4, 1.6]	< 1.0
All	25%	75%	0%
$22 \leq r \leq 24$	13%	87%	0%
$r \geq 24$	0%	17%	83%

According to the definition of blue population by BO, the lack of E/S0 galaxies in this cluster gives a value of f_B close to 1. The number of galaxies with $M_V < -20$ (equivalent to $r < 22.7$ for elliptical galaxies at $z = 0.540$) is only 70 within the cutoff radius of the cluster (Sect. 5.2), and 10 within R_{30} (= 26″, see Sect. 5.2). The contamination level, as estimated from the comparison field, is close to 10%. Almost all these objects are at least 0.2 mag bluer than a typical E galaxy in B − g and g − r, so the fraction of blue objects inferred is very high: $f_B = 0.8 \pm 0.5$. The result is the same when the sample is limited to galaxies within the completeness magnitude in g ($g \leq 24.5$). In this case there are 10 galaxies within R_{30}, 9 of which are "blue", with a contamination level close to 50%.

Fig. 8. Color–color diagrams in the field of Cl 1600+4109 and in the comparison field. Three magnitude intervals are considered: **a and b** $r \leq 22$, **c and d** $22 < r < 24$, **e and f** $r \geq 24$. Objects are identified as in Fig. 7. The colors predicted for the different types of galaxies at $z = 0.540$, from E to Im, and the typical error boxes in each magnitude bin are also shown

5.2. The 2D distribution of galaxies

The shape of Cl 1600+4109 is obtained from the projected number density of galaxies. Figure 9 shows the isocontour map. The ellipticity of the cluster is $\epsilon \simeq 0.75$ and the position angle $\theta \simeq 45°$. The cluster is dominated by a small group of galaxies in its central part (see Fig. 2 in Paper I). There is a bright galaxy of magnitude r = 19.58 in the center of the group, with colors fully compatible with those expected for an elliptical galaxy at $z = 0.540$.

The cluster profile and the cutoff radius have been calculated as in Cl 1613+3104, using the projected density of the comparison field. The cutoff radius is 78″ (635 h^{-1} kpc); the total number of objects within it is 137, and there are 100 objects in the comparison field, under the same conditions. most objects in excess with respect to the empty field are found beyond the completeness limit in magnitude in the three filters. We have obtained an estimate of the concentration parameters without introducing any selection in magnitude. The concentration parameter is C = 0.40, with R_{30} = 26″ (212 h^{-1} kpc) and N_{30} = 10. The central galaxy density, $N_{0.5}$, is

strongly dependent on the filter used. The highest value is attained in the B filter, with $N_{0.5} = 20$, as expected for a so blue population of galaxies. The corresponding velocity dispersion (Bahcall 1981) is about 800–1000 km s^{-1}. These values of $N_{0.5}$ and C should only be taken as a rough estimate, because the sample has not been limited in magnitude. The projected galaxy density profile, according to Eq. (2) with $\alpha \equiv 1$, is: $\sigma_0 = 0.008 \pm 0.002$ gal $arcsec^{-2}$ and $R_c = 12'' \pm 8''$ (100 ± 70 h^{-1} kpc).

Fig. 9. Isocontour map of the projected number density of galaxies in the field of Cl 1600+4109. The mean projected density over the cluster field is 5.0×10^{-3}objects $arcsec^{-2}$, and the difference between two successive contour levels is 0.5 times the mean density, starting at 1. X and Y coordinates are in arcsec, with the center of the cluster at ($80''$, $130''$)

The λ_n-method does not detect any obvious segregation either in magnitude or in color. There is a slight tendency among red objects to be more concentrated than blue objects, but this trend is of the same order as the errors.

6. Discussion and conclusions

Cl 1613+3104 is a rich, concentrated cluster, dominated by a compact group of luminous galaxies within a radius of 121 h^{-1} kpc around the center. The cluster shows strong evidence for segregation in luminosity and color, and both effects seem to be independent. Red and bright objects tend to concentrate around the center of the cluster. The distribution of galaxies in colors shows two different populations of objects. The red population is compatible with the colors expected for E/S0 type galaxies at the cluster redshift. These objects dominate the population of cluster galaxies at low magnitudes and they are located preferentially in the central part of the cluster. The blue population is explained in part by the presence of normal star-forming S/Im galaxies, but a population of galaxies bluer than normal Im galaxies at the cluster redshift is also detected. Moreover, the 2D distribution for the red population is clearly more concentrated around the center of the cluster than the blue one.

The detection level in Cl 1600+4109 is lower than in Cl 1613+3104, and most cluster galaxies are found beyond the completeness limits in magnitude. Nevertheless, its concentration and richness parameters indicate that we are probably dealing with a rich, concentrated cluster. It is dominated by a bright galaxy in its central region, with colors fully compatible with those expected for E galaxies at this redshift. The fraction of E/S0 galaxies is low in this cluster (less than 15% within the completeness limit in r), and the population of galaxies is dominated by S/Im galaxies. There is no evidence of segregation in magnitude or in color.

In both clusters, the luminosity function in B is compatible with the standard values derived by Colless (1989) for a sample of rich low-redshift clusters. The absolute magnitudes derived for their brightest galaxies, after applying the standard k+e correction, are similar. The main galaxy in Cl 1600+4109 is slightly brighter than that of Cl 1613+3104 ($M_r = -23.40$ compared to $M_r = -23.01$, within the isophote corresponding to 1σ of the background sky noise). Comparison of the two histograms in M_B for Cl 1600+4109 and Cl 1613+3104, after correction through the comparison field (Figs. 1 and 6), shows that the completeness magnitude in Cl 1613+3104 is 1.2 mag fainter than in Cl 1600+4109 when a k correction for E/S0 galaxies is used, and this value reduces to 0.9 mag when a standard k+e correction is applied. Nevertheless, most galaxies with magnitudes around B_{com} in both clusters are S/Im galaxies. When the k correction used is that of an Sb galaxy, the completeness magnitude in Cl 1613+3104 is 0.6 mag fainter than in Cl 1600+4109, and the difference reduces to 0.3 mag after a k+e correction. So the absolute detection level in Cl 1600+4109 is poorer than in Cl 1613+3104. The main reason for this is probably the difference in the seeing conditions between both clusters. Cl 1613+3104 was observed with an averaged seeing of $\sim 1''.3$, whereas the seeing was $\sim 2''.1$ for Cl 1600+4109, but the isophotes used to integrate fluxes were 0.5 mag fainter in the later (see Paper I). A straightforward simulation of photometry has been done, taking the best r image of Cl 1613+3104 (seeing = $1''.1$) and debasing it to an equivalent seeing of $\sim 2''.5$. As expected, a general tendency appears in the isophotal magnitudes: objects in the bad-seeing image tend to be measured as fainter than in the good-seeing one, and this effect increases with the magnitude. The brightest objects ($r \lesssim 20$), such as the main cluster-galaxies, are almost unaffected, the difference being lower than 0.1 mag. This difference is about 0.2 mag for objects with $r \simeq 23$, and it increases to 0.4 mag for the faintest objects in the sample, up to $r = 25$. Using a fainter isophote to integrate magnitudes, as it was done for Cl 1600+4109, strongly reduces the effect. When the isophotal magnitude is the same in both the good and the bad seeing images, the difference in magnitude for the faintest objects can be as large as 0.7 to 1 mag.

In Cl 1613+3104, the population of galaxies is dominated by the E/S0 type, at least up to the completeness limit in r. In the case of Cl 1600+4109, there is a lack of E/S0 galaxies (they are less than 15% of the sample) and the population is mainly composed of S/Im galaxies up the completeness limit in r. The extremely blue population dominates the sample at faint magnitudes ($r > 24$) in both clusters. The general trend is that the fraction of blue galaxies in excess with respect to an empty field increases with magnitude. Nevertheless, getting the abso-

Table 3. Expected colors for a single burst of star formation as a function of its age, as seen at the redshifts of both clusters

Age [log(yr)]	B − r [$z = 0.415$]	g − r	B − r [$z = 0.540$]	g − r
5	−0.10	0.04	−0.06	0.08
6	−0.13	0.02	−0.09	0.06
7	0.32	0.40	0.27	0.36
8	0.85	0.83	0.87	0.86
9	1.44	1.30	1.51	1.36

lute distribution in morphological types is only possible when the sample of galaxies is limited within the magnitude of completeness in *all* the filters involved. Otherwise, a bias is introduced, as can be seen in Figs. 2 and 7. The result is that the fraction of blue objects detected in both clusters should be considered as an upper bound because the detection of red objects is not complete. In Cl 1613+3104, the color-color diagrams are only complete for objects bluer than B − r = 0.25 and g − r = 0.5 in the interval 22 ≤ r ≤ 24 and B − r = −0.5 and g − r = −0.25 when r ≥ 24. In Cl 1600+4109, this condition is fulfilled for objects bluer than B − r = 0.75 and g − r = 0.75 if 22 ≤ r ≤ 24, and B − r = −0.25 and g − r = −0.25 when r ≥ 24. However, even if the absolute ratio of blue to red objects is biased, the both cluster fields show clearly an excess of extremely blue objects in comparison with an empty field, and the number of such objects increases with the magnitude. Table 3 gives the location in the color-color plane of a single burst of star formation, as seen at the redshifts of both clusters, as a function of its age. It is assumed that the light coming from the stellar mass created by the burst is responsible for the bulk of the energy in the spectra. When we compare these values with the color-color distributions shown in Figs. 3 and 8, it appears that most extremely blue objects in both clusters are compatible with the colors expected for such burst models younger than a few 10^7 yr. High quality images of these clusters could confirm the hypothesis that these galaxies are going through mergers or tidal interactions. These observations would reinforce the idea that triggers of starburst processes were more frequent in the past than in the present epoch.

Acknowledgements. We wish to thank the technical staff of the CAHA for his help during the photometric runs at the 3.5 m telescope. We are grateful to J.-F. Le Borgne for his help during the data reduction. We wish to thank G. Bruzual for allowing the use of his code for the spectral evolution of galaxies. This work has been supported by the Spanish DGICYT program PB90-0448 of the *Ministerio de Educación y Ciencia* and, partially, by the Human Capital and Mobility Programme (EU), under contract CHRX-CT92-0044.

References

Bahcall N.A., 1981, ApJ 247, 787
Bruzual G., Charlot S., 1993, ApJ 405, 538
Burstein D., Heiles C., 1982, AJ 87, 1165
Butcher H., Oemler A., 1978, ApJ 226, 559
Butcher H., Oemler A., 1984, ApJ 285, 426 (BO)
Capelato H.V., Gerbal D., Mathez G., et al., 1980, ApJ 241, 521
Cardelli J.A., Clayton G.C., Mathis J.S., 1989, ApJ 345, 245
Colles M., 1989, MNRAS 237, 799
Couch W.J., Ellis R.S., Sharples R.M., Smail I., 1994, ApJ 430, 121
Dressler, A., Gunn J.E., 1992, ApJS 78, 1
Dressler A., Gunn J.E., Schneider D.P., 1985, ApJ 294, 70
Dressler A., Oemler A., Butcher H.R., Gunn J.E., 1994a, ApJ 430, 107
Dressler A., Oemler A., Sparks W.B., Lucas R.A., 1994b, ApJ 435, L23
Gunn J.E., Hoessel J.G., Oke J.B., 1986, ApJ 306, 30
Henry J.P., Soltan A., Briel U., Gunn J.E., 1982, ApJ 262, 1
Hickson P., 1977, ApJ 217, 16
Jaffe W., 1982, ApJ 262, 15
Mellier Y., Soucail G., Fort B., Mathez G., 1988, A&A 199, 13
Miller G.E., Scalo J.M., 1979, ApJS 41, 513
Pelló R., Vílchez–Gómez R., 1996, A&AS 115, 1 (Paper I)
Rocca–Volmerange B., Guiderdoni B., 1988, A&AS 75, 93
Sandage A., Kristian J., Westphal J.A., 1976, ApJ 205, 688
Schechter P., 1976, ApJ 203, 297
Sharples R.M., Ellis R.S., Couch W.J., Gray P., 1985, MNRAS 212, 687
Thuan T.X., Gunn J.E., 1976, PASP 88, 543
Vílchez–Gómez R., Pelló R., Sanahuja B., 1994, A&A 283, 37 (Erratum: 1994, A&A 289, 661)
Zwicky F., Herzog E., Wild P., Karpowicz M., Kowal C.T., 1961–1968, Catalogue of Galaxies and Clusters of Galaxies. California Institute of Technology, Pasadena

This article was processed by the author using Springer-Verlag LaTeX A&A style file *L-AA* version 3.

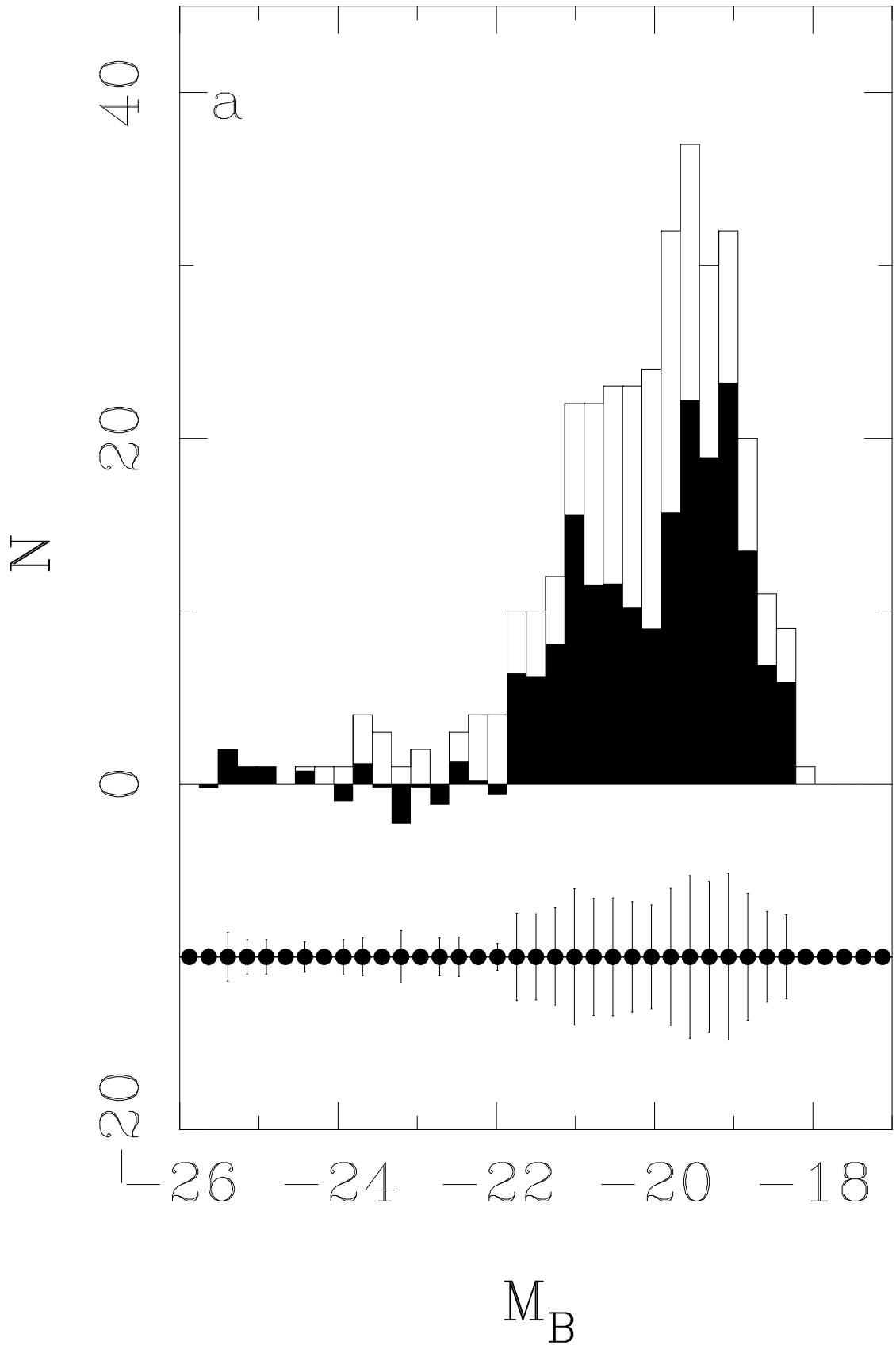
a
40
20
0
−20
N
−26
−24
−22
−20
−18
M_B

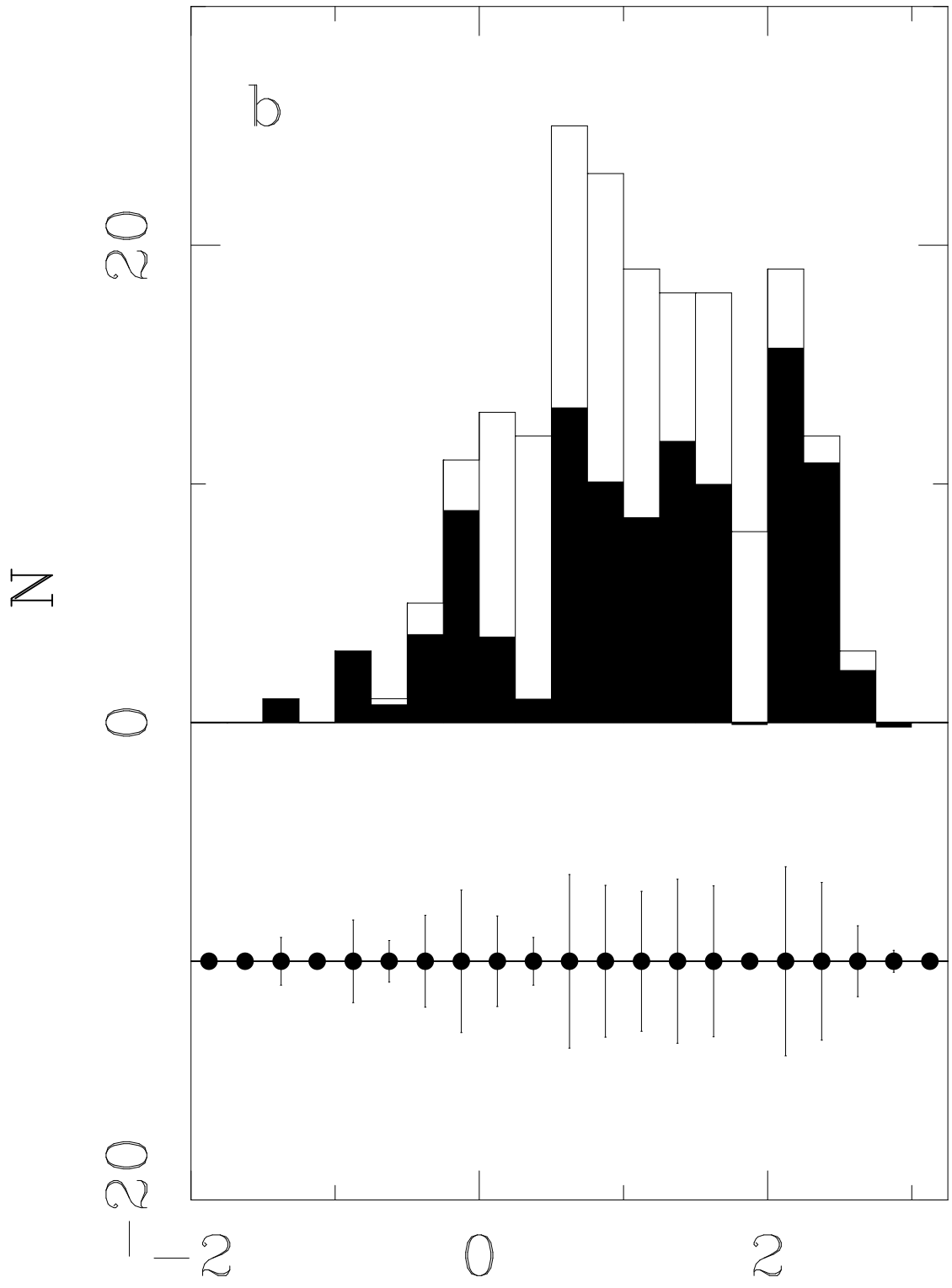
b
N
20
0
−20
−2
0
2
B − r

c
N
40
20
0
−20
−2
0
2
g − r

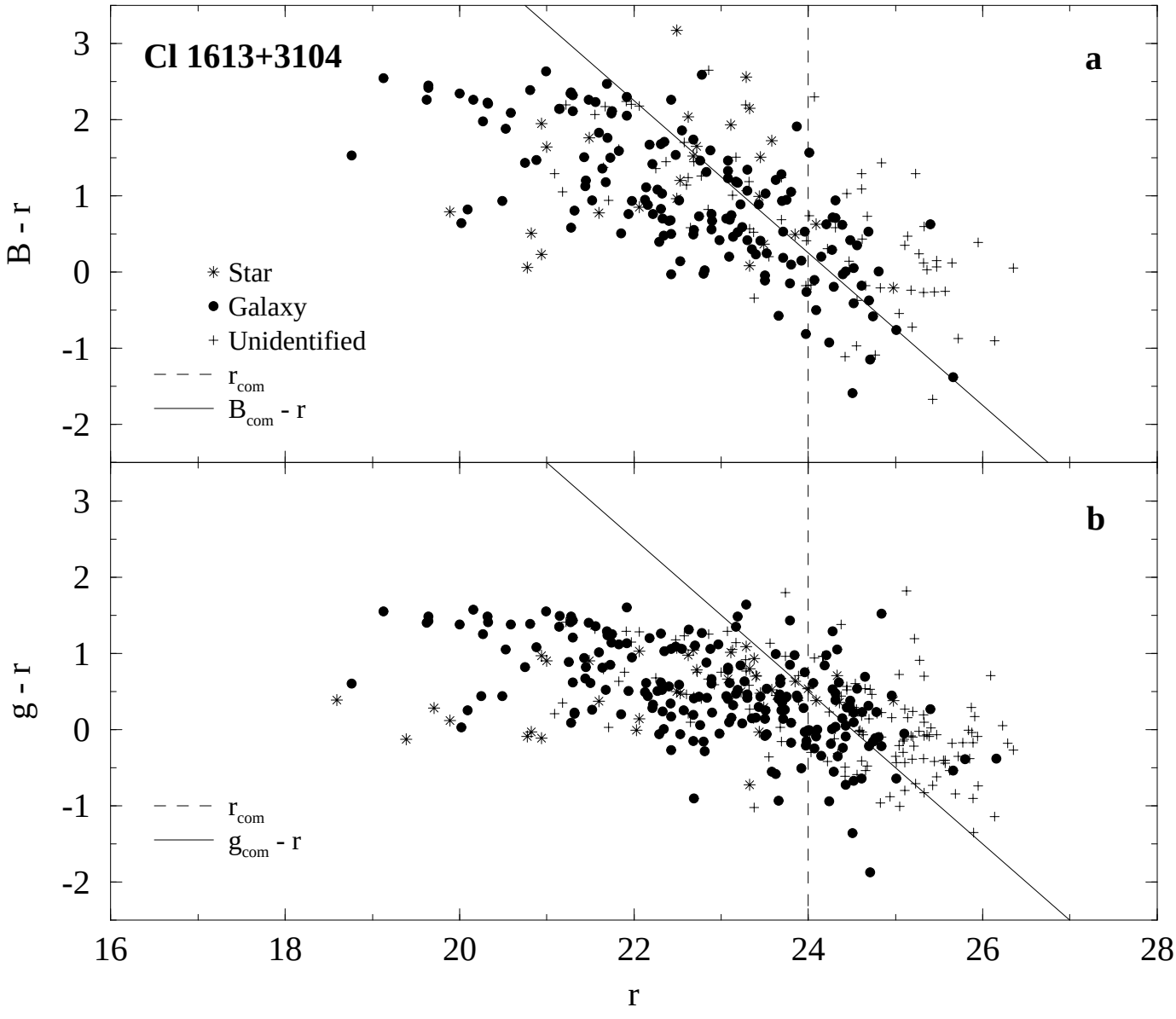
Cl 1613+3104
a
b
B - r
g - r
r
Star
Galaxy
Unidentified
r_com
B_com - r
g_com - r
3
2
1
0
-1
-2
16
18
20
22
24
26
28

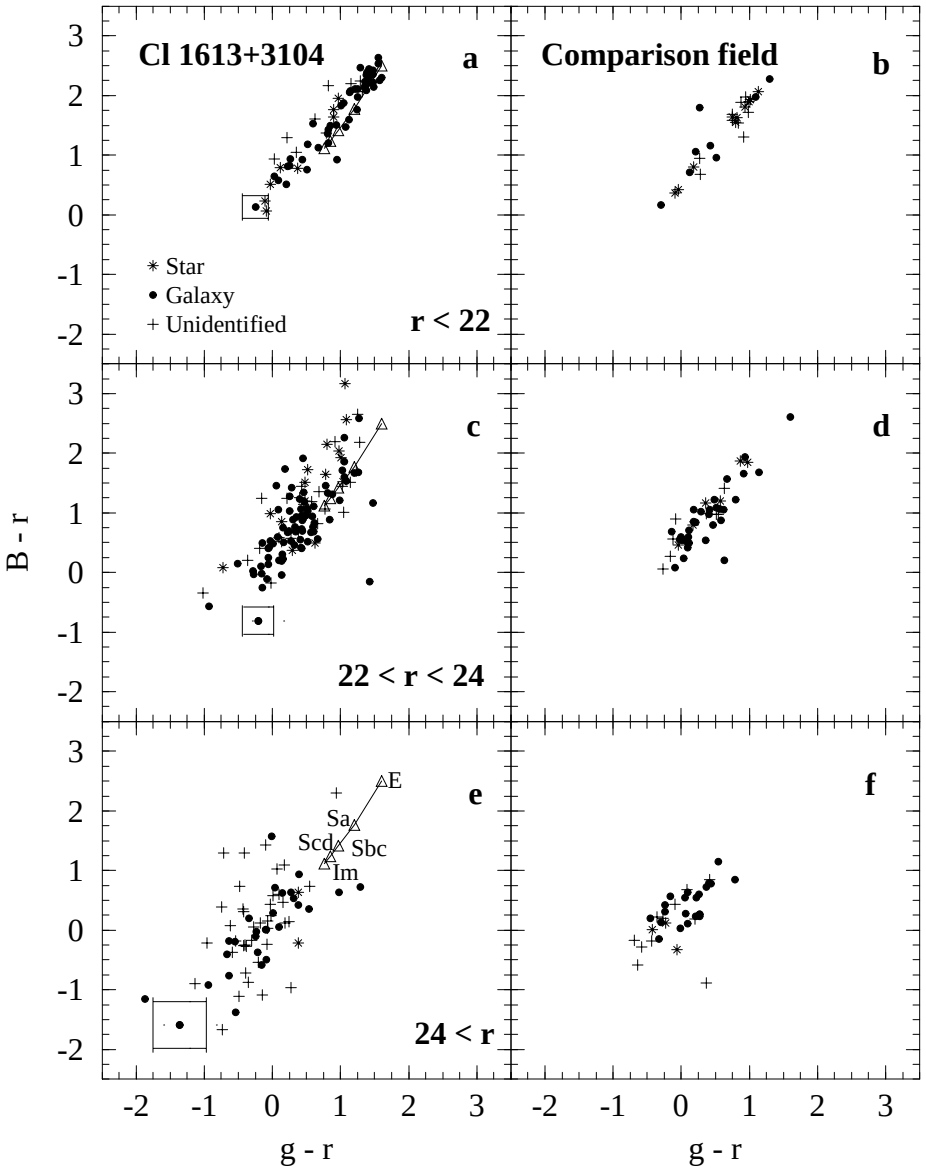
Cl 1613+3104
a
Comparison field
b
Star
Galaxy
Unidentified
r < 22
c
d
22 < r < 24
e
f
E
Sa
Scd
Sbc
Im
24 < r
B - r
g - r
g - r

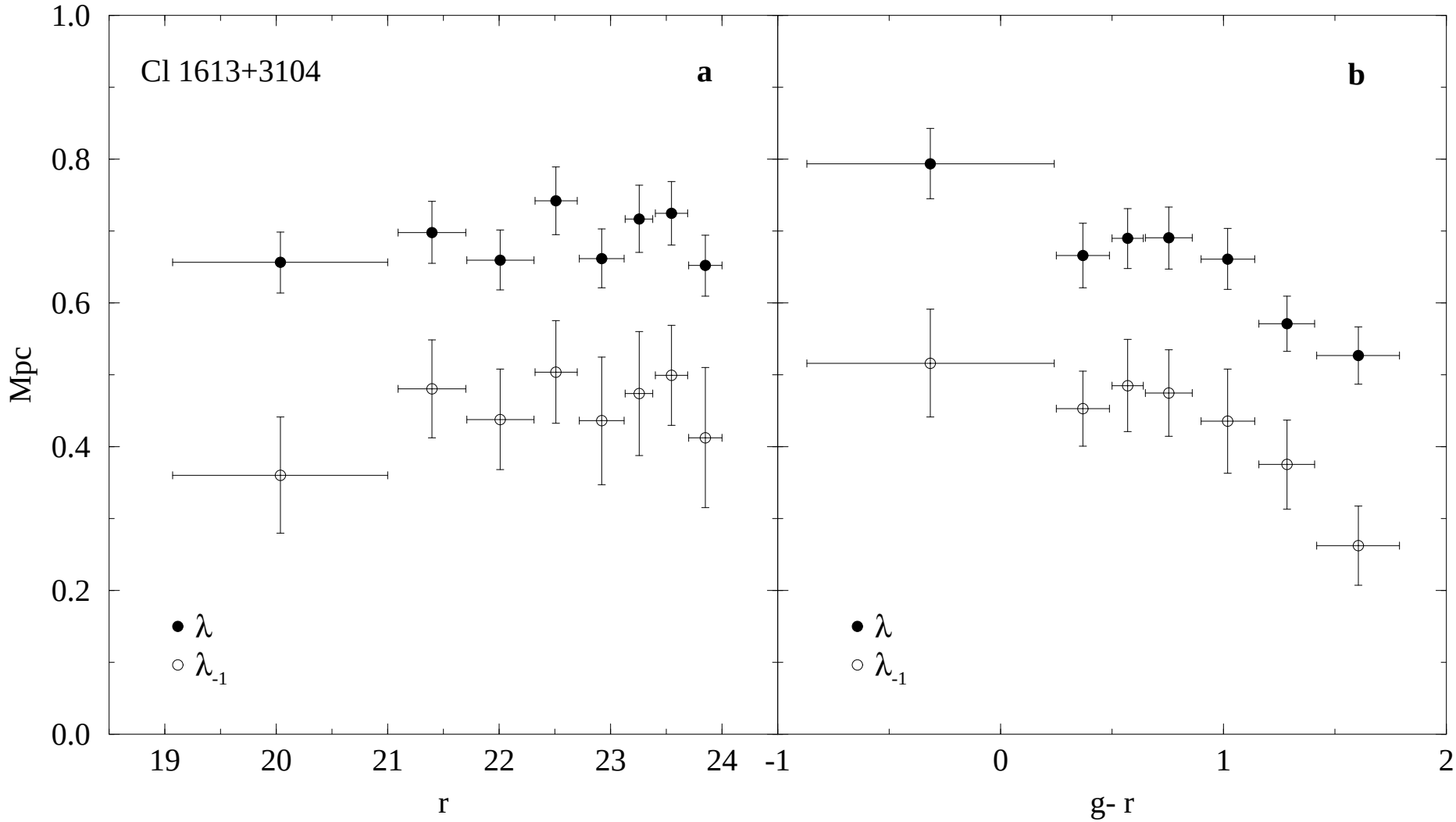
Cl 1613+3104
a
b
Mpc
r
g- r
λ
λ-1
1.0
0.8
0.6
0.4
0.2
0.0
19
20
21
22
23
24
-1
0
1
2

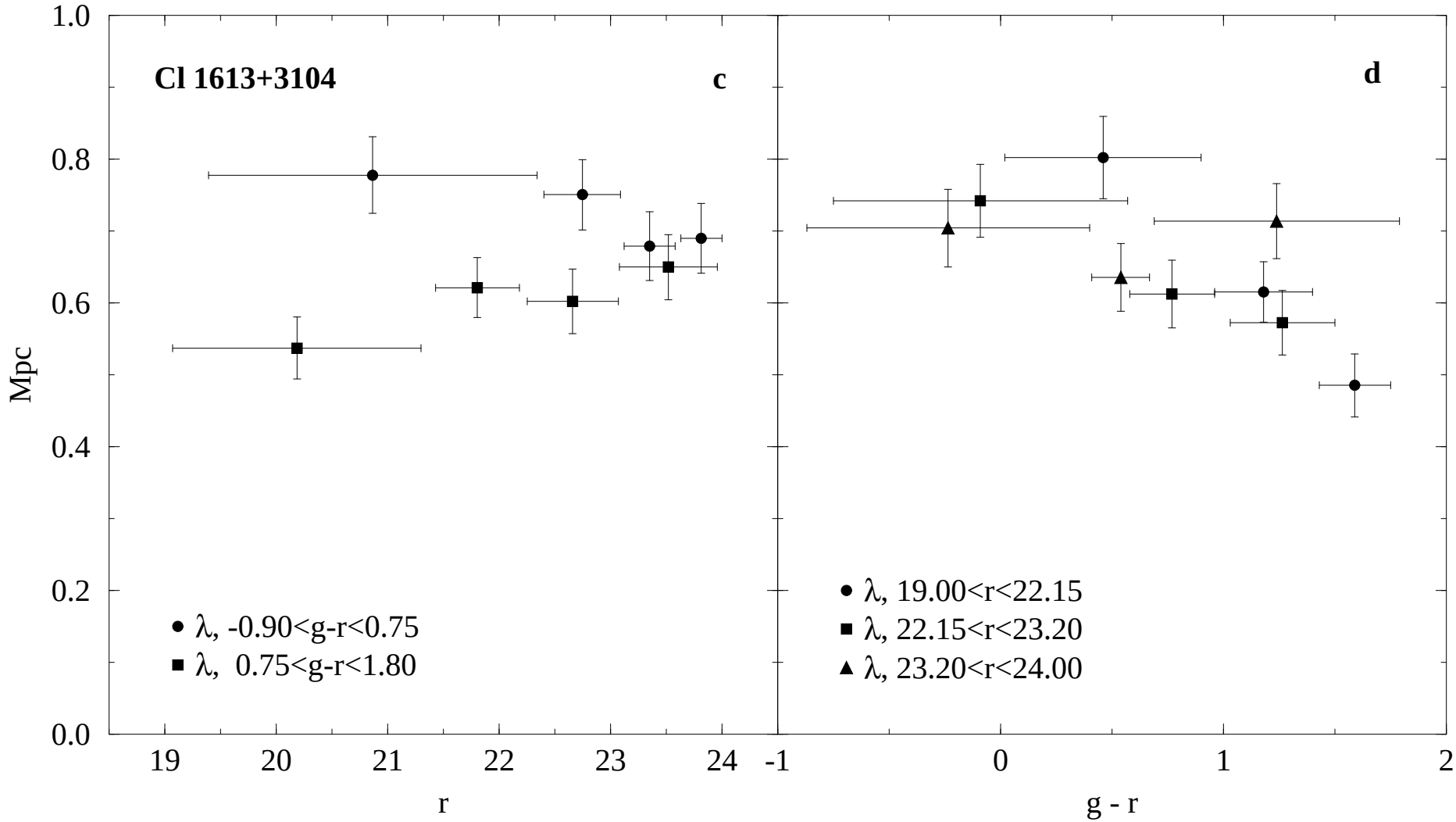
Cl 1613+3104
c
d
Mpc
r
g - r
λ, -0.90<g-r<0.75
λ, 0.75<g-r<1.80
λ, 19.00<r<22.15
λ, 22.15<r<23.20
λ, 23.20<r<24.00
1.0
0.8
0.6
0.4
0.2
0.0
19
20
21
22
23
24
-1
0
1
2

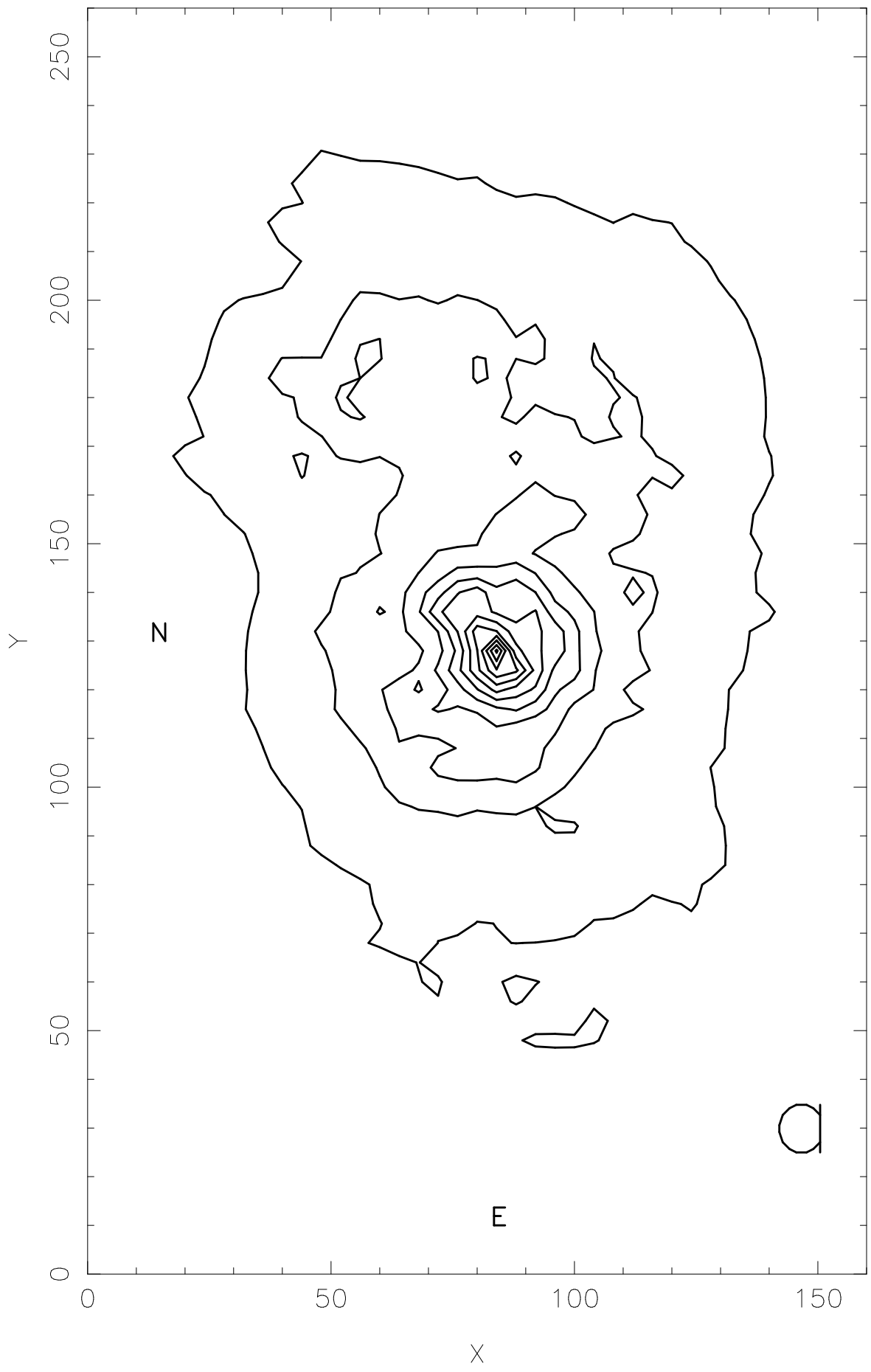
Cl1613+3104 Red Population
250
200
150
100
50
0
Y
N
E
a
0
50
100
150
X

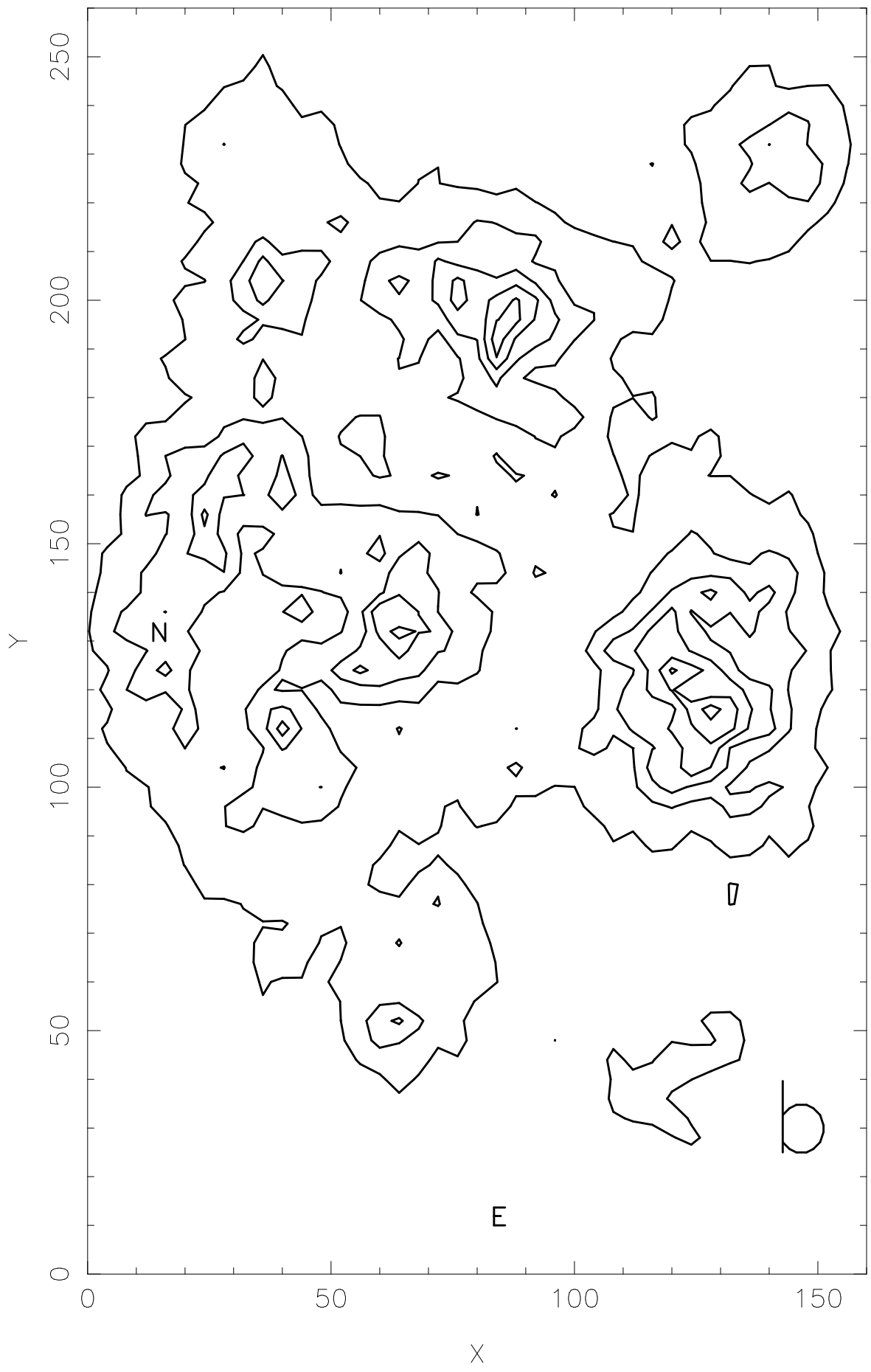
Cl1613+3104 Blue Population
250
200
150
100
50
0
Y
0
50
100
150
X
N
E
b

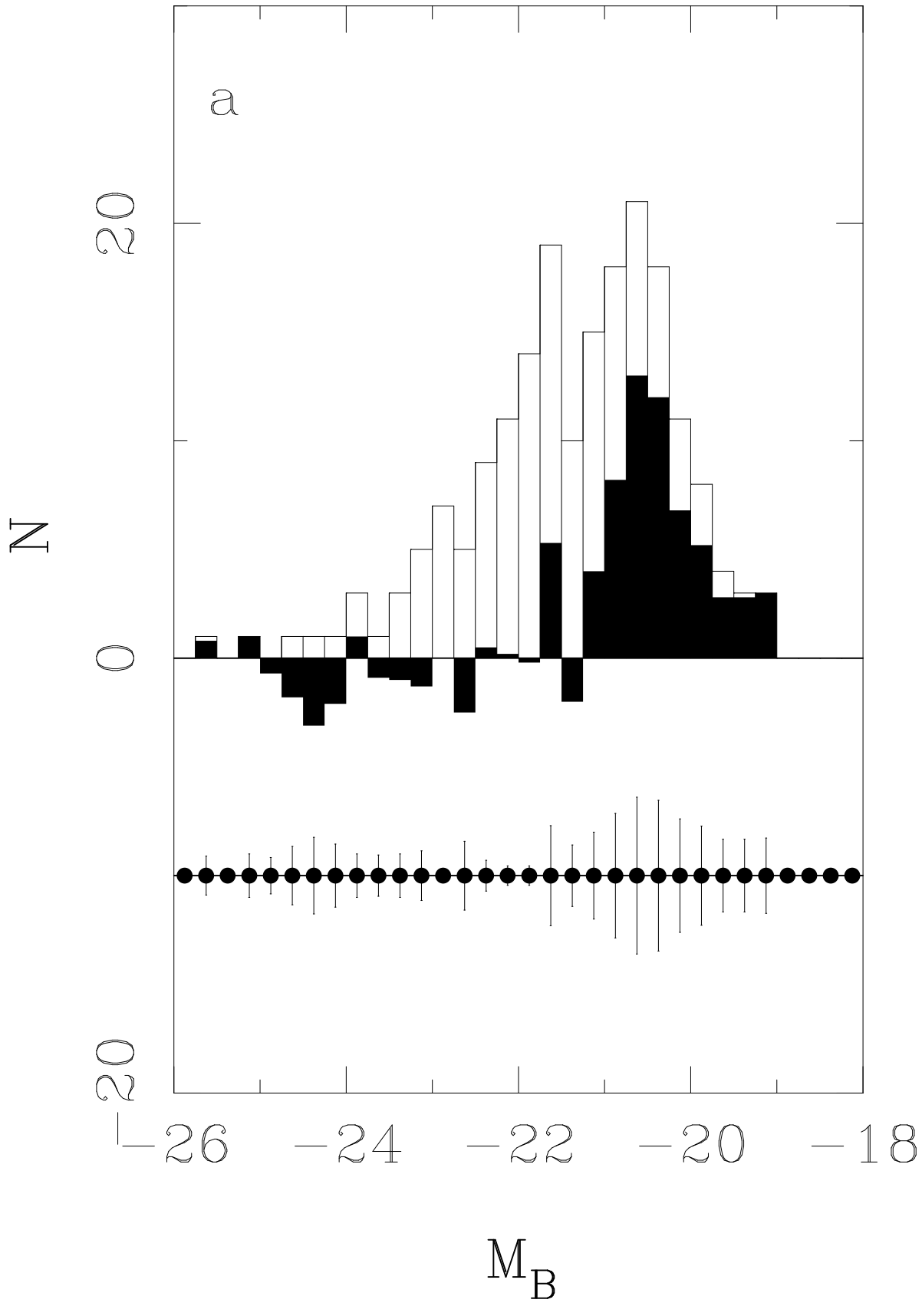
a
20
0
20
N
−26
−24
−22
−20
−18
M_B

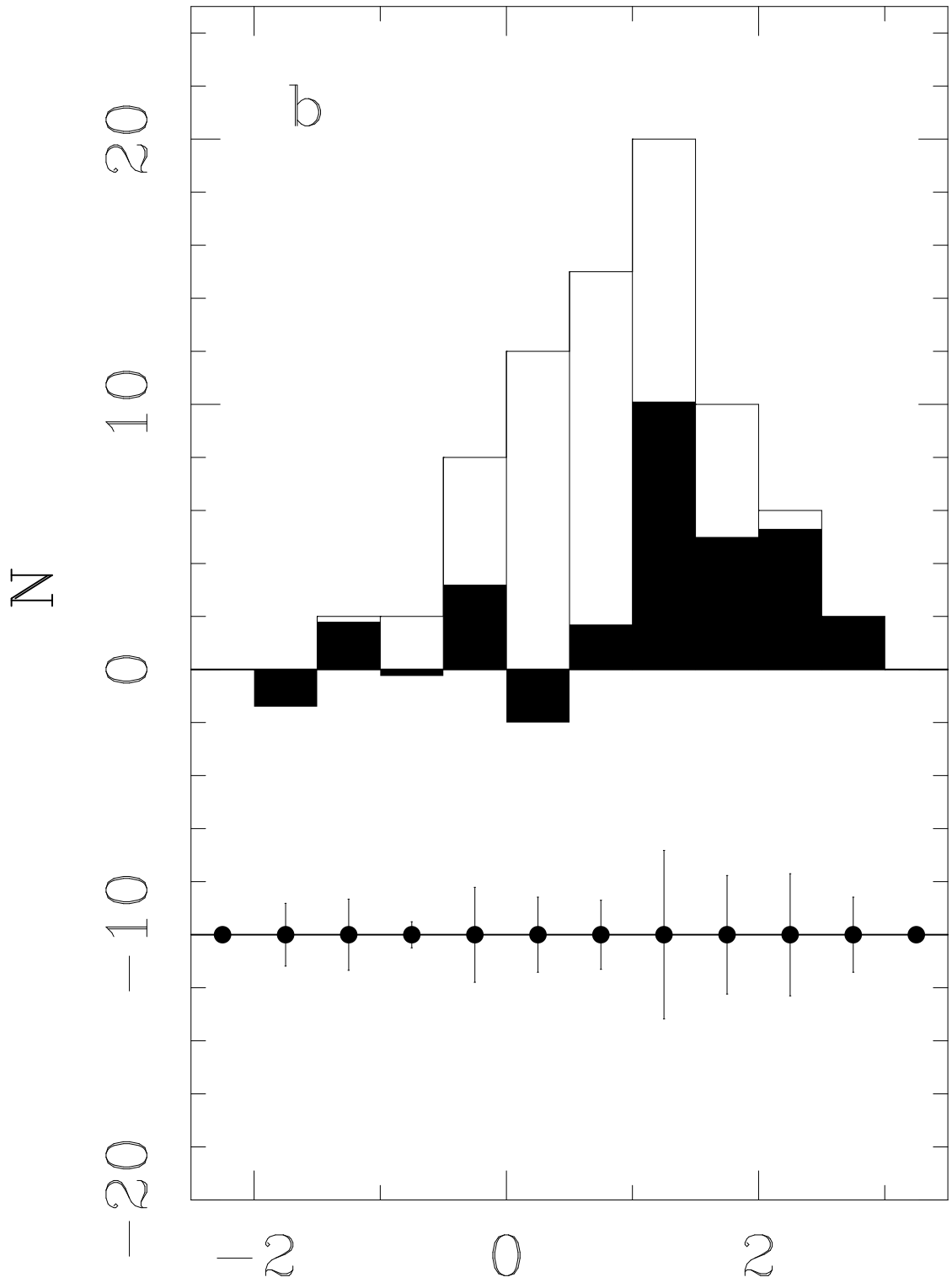
b
N
20
10
0
−10
−20
−2
0
2
B − r

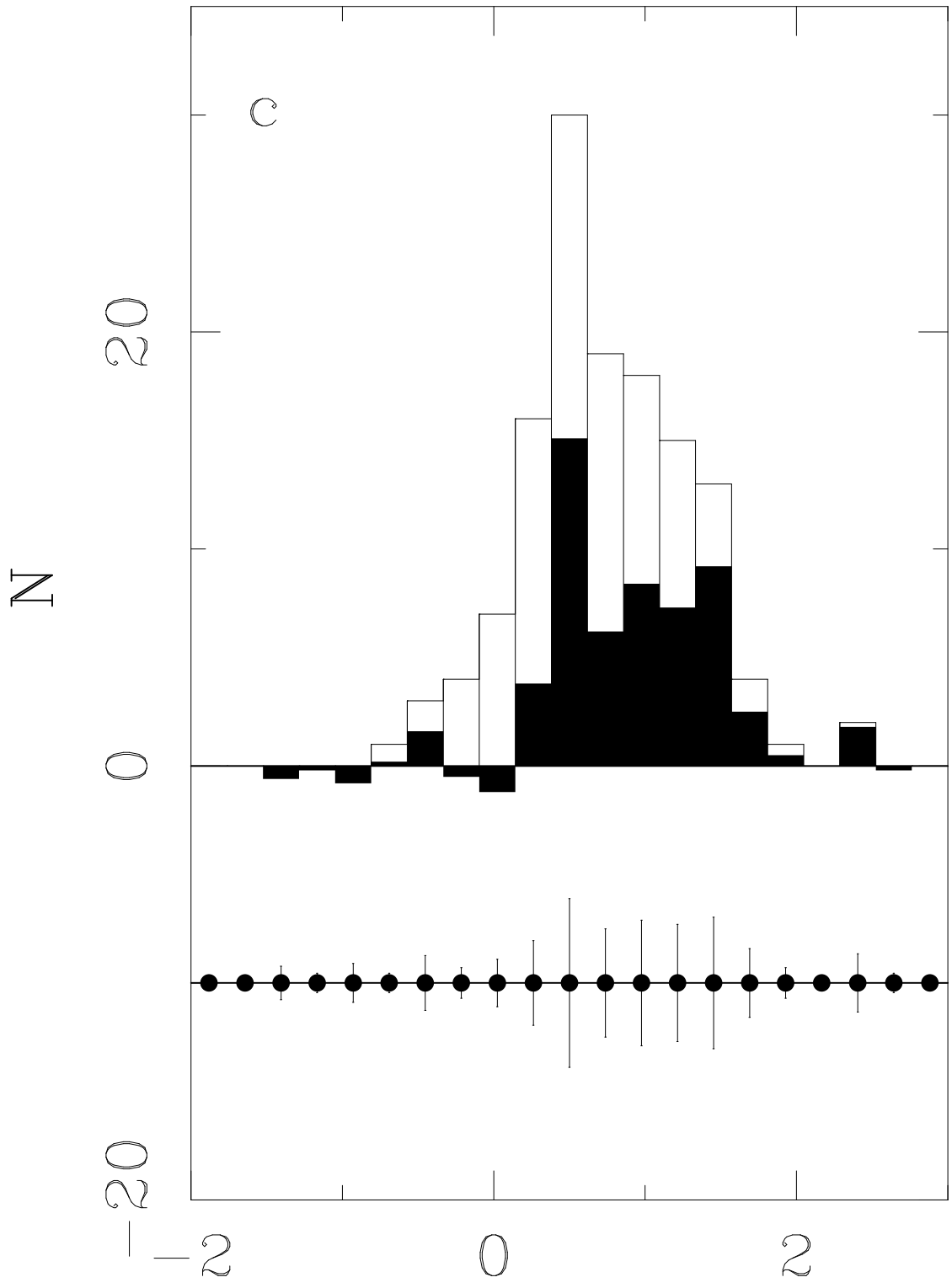
c
N
20
0
−20
−2
0
2
g − r

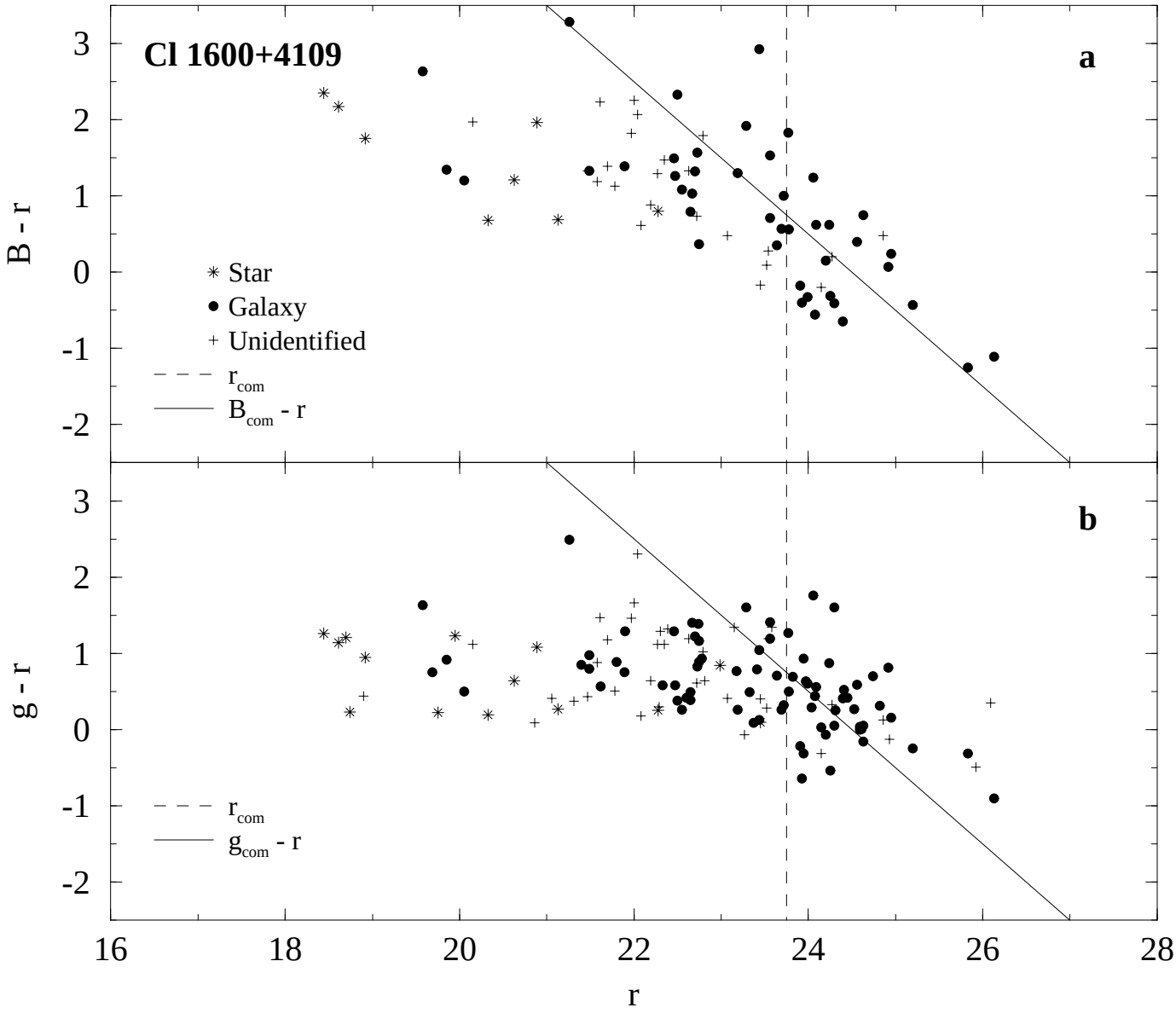
Cl 1600+4109
a
b
B - r
g - r
Star
Galaxy
Unidentified
r_com
B_com - r
g_com - r
r
3
2
1
0
-1
-2
16
18
20
22
24
26
28

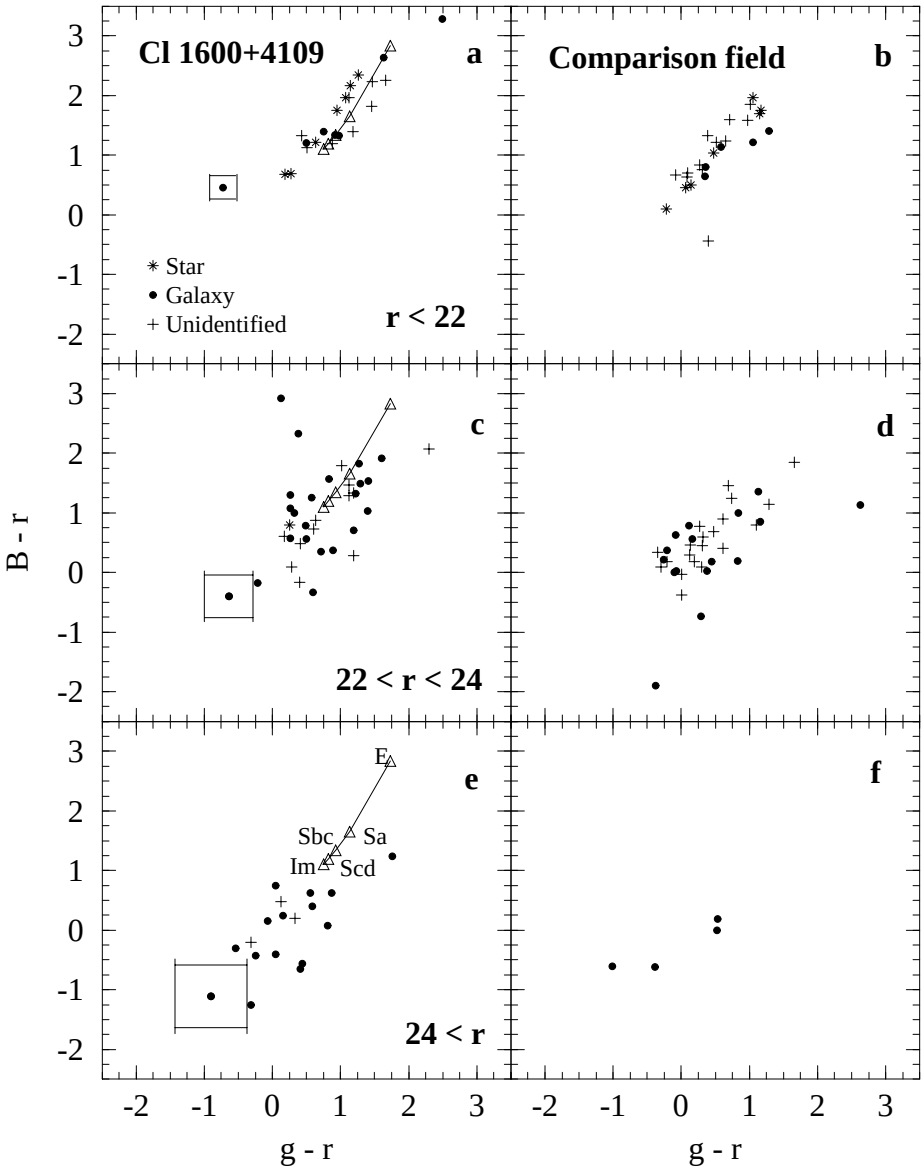
Cl 1600+4109
a
Comparison field
b
Star
Galaxy
Unidentified
r < 22
c
d
22 < r < 24
E
e
f
Sbc
Sa
Im
Scd
24 < r
B - r
g - r
g - r

Cl1600+4109